Progress of Theoretical Physics, Vol. 96, No. 2, August 1996

Instability of Synchronized Binary Neutron Stars in the First Post-Newtonian Approximation of General Relativity

Masaru SHIBATA

Department of Earth and Space Science
Faculty of Science, Osaka University, Toyonaka 560

(Received March 27, 1996)

We investigate the stability property of binary neutron stars (BNSs) just before the merging in the first post-Newtonian(PN) approximation. Stability analysis is performed making use of equilibrium configurations for synchronized BNSs which are obtained by the numerical scheme developed in a previous paper. NSs are modeled by means of the polytropic equation of state with the polytropic exponent $\Gamma=2$ and 3. From numerical calculations, we find that as in the Newtonian case, in the PN approximation, the secular instability will occur for synchronized BNSs at a critical angular velocity $\Omega_{\rm crit}$ before the surfaces of the two stars come into contact. The PN correction changes not only the gravitational attraction force between two NSs, but also the configuration of each NS of a binary system. As a result, $\Omega_{\rm crit}$ in the PN approximation is $\sim 10-15\,\%$ larger than that in the Newtonian case for a NS of mass $M_{\rm ADM}\sim 1.4\,M_\odot$ and radius $r_A\sim 10-15$ km. The implication of this property to the orbital evolution of BNSs just before merging is discussed.

§ 1. Introduction

The last stage of coalescing binary neutron stars (BNSs), in which gravitational waves of frequency $10-1000$ Hz are emitted, is one of the most promising sources of gravitational waves for kilo meter size laser interferometric detectors such as LIGO[1] and VIRGO.[2] Evolutions of these compact BNSs are as follows: When the orbital separation of BNSs is sufficiently large compared with the NS radius, BNSs evolve in an adiabatic manner, radiating gravitational waves on a much longer time scale than the orbital period, because the general relativistic (GR) gravity is not particularly strong. In such an inspiraling phase, they can also be regarded approximately as two point masses, because the hydrodynamic effect is not important.[3),4)] On the other hand, when the orbital separation of BNSs becomes comparable to the NS radius, the hydrodynamic effect becomes important for the evolution of BNSs, and also the GR gravity becomes very strong. In such a phase, NSs do not behave as point masses, and also the binary evolves not in the adiabatic manner, but in the dynamical manner to merge.

These evolution scenarios imply that the nature of the signal of gravitational waves changes around a transition region between the inspiraling and merging phases. Gravitational waves emitted at this transition region carry important information about the NS radius,[4),5)] which can be used to determine the equation of state (EOS) of NS matter.[6)] Thus, investigations of gravitational waves in the merging phase, in particular, around the transition region from the inspiraling phase to the merging phase are very important. The purpose of this paper is to investigate the transition region incorporating the GR effect as well as the hydrodynamic effect.

As a trigger of the transition, recently, the tidal effect was pointed out by Lai et al.:[7),8)] They showed that when the orbital separation of BNSs becomes small, each star of binary system is significantly deformed by the tidal force of the companion star. In such a case, a tidal field due to the deformation of each star is generated,[9)] and as a result the circular orbit of the BNSs becomes unstable.

When we consider the tidal effect in the binary system, we need to know the configuration of each star, because the tidal effect on each star depends on its structure. Thus, when we consider the tidal effect on BNSs, we must take into account GR effects because GR gravity plays an important role in determining the configuration of a NS. This means that in order to know whether the tidal effect is important or not, we must investigate the evolution of BNSs just before the merging, taking into account not only the hydrodynamic effect, but also the effect of the GR gravity on each star of a binary system. For this purpose, we perform the PN calculation to obtain equilibrium configurations for *synchronized* BNSs in circular orbits and investigate the stability property of BNSs.

As pointed out by Kochanek, and Bildsten and Cutler,[10)] the synchronization of BNSs is realized only when the viscosity of the NS matter is extremely large and the circulation of the system is effectively dissipated. Hence, in order to understand the stability property for realistic BNSs, we must investigate BNSs in non-synchronized orbits, taking into account the case where the circulation of the system is approximately conserved.[10)] However, we do not have a numerical method of obtaining accurately the equilibrium configuration of non-synchronized BNSs, in contrast to the case of synchronized BNSs. Fortunately, the stability property of the non-synchronized binary seems to be similar to that of the synchronized one in the Newtonian case, as shown by Lai et al.[7),8)] Therefore, investigation of the stability property of synchronized BNSs should be a guideline for that of other types of BNSs.

This paper is organized as follows. In § 2, we briefly show the basic equations for obtaining the PN configuration of uniformly rotating bodies, and define various quantities in the first PN approximation. In § 3, we show numerical results for synchronized BNSs in circular orbits. Paying attention to the angular momentum and energy of the binary systems as a function of the orbital separation, we investigate the stability property of BNSs just before the merging, and the GR effect on it. Section 4 is devoted to a summary. Throughout this paper, c and G, respectively, denote the speed of light and the gravitational constant.

§ 2. Basic equations

As shown in a previous paper,[12)] in the first PN approximation, the equilibrium configuration for a uniformly rotating self-gravitating system of a polytropic EOS,

$$P=(\Gamma-1)\rho\varepsilon=K\rho^{\Gamma}\,, \tag{2·1}$$

is obtained from the following sets of equations:[11),12)]

$$\frac{K\Gamma}{\Gamma-1}\rho^{\Gamma-1}-\frac{1}{2c^2}\left(\frac{K\Gamma}{\Gamma-1}\rho^{\Gamma-1}\right)^2$$

$$=U-\frac{X_0}{c^2}+\left\{\frac{R^2}{2}+\frac{1}{c^2}(2R^2U-X_\Omega+\hat{\beta}_\varphi)\right\}\Omega^2+\frac{R^4}{4c^2}\Omega^4+\text{const}\,, \tag{2·2}$$

and

$$\Delta U=-4\pi G\rho\,, \tag{2·3}$$

$$\Delta\hat{P}_1=-4\pi G\rho x\,, \tag{2·4}$$

$$\Delta\hat{P}_2=-4\pi G\rho y\,, \tag{2·5}$$

$$\Delta X_0=4\pi G\rho\left(\varepsilon+2U+\frac{3P}{\rho}\right), \tag{2·6}$$

$$\Delta X_\Omega=8\pi G\rho R^2\,, \tag{2·7}$$

where ρ, ε, P, K, Γ and Ω denote the mass density, the specific internal energy, the pressure, the polytropic constant, the polytropic exponent, and the angular velocity $(d\varphi/dt)$, respectively. R^2 denotes x^2+y^2, and $\hat{\beta}_\varphi$ is given by

$$\hat{\beta}_\varphi=-\left[\frac{7}{2}(x\hat{P}_1+y\hat{P}_2)+\frac{1}{2}(x^2\hat{P}_{2,y}+y^2\hat{P}_{1,x}-xy\hat{P}_{1,y}-xy\hat{P}_{2,x})\right]. \tag{2·8}$$

In this paper, we will obtain the equilibrium configuration of BNSs of equal masses. The numerical method of obtaining these configurations is the same as that in a previous paper.[12] To solve the Poisson equations numerically, we use the Cartesian coordinate and take a homogeneous grid with grid number $(N_x, N_y, N_z)=(89, 89, 45)$.

In the first PN approximation, we have the following conserved quantities:

(1) the conserved mass

$$M_*=\int\rho_* d^3x\,, \tag{2·9}$$

where ρ_* is the conserved mass density, which is defined as

$$\rho_*=\rho\left\{1+\frac{1}{c^2}\left(\frac{v^2}{2}+3U\right)\right\} \tag{2·10}$$

and $v^2=R^2\Omega^2$,

(2) the ADM mass

$$M_{\rm ADM}=\int\rho\left\{1+\frac{1}{c^2}\left(v^2+\frac{5}{2}U+\varepsilon\right)\right\}d^3x\,, \tag{2·11}$$

(3) the total energy[13]

$$E=\int\rho\left\{\varepsilon+\frac{v^2}{2}-\frac{1}{2}U+\frac{1}{c^2}\left(\frac{5}{8}v^4+\frac{5}{2}v^2U+\frac{1}{2}\Omega^2\hat{\beta}_\varphi+\varepsilon v^2+\frac{P}{\rho}v^2+2\varepsilon U-\frac{5}{2}U^2\right)\right\}d^3x\,, \tag{2·12}$$

and

(4) the total angular momentum[13)]

$$J=\Omega\int\rho\Big[R^2\Big\{1+\frac{1}{c^2}\Big(v^2+6U+\varepsilon+\frac{P}{\rho}\Big)\Big\}+\frac{\hat{\beta}_\varphi}{c^2}\Big]d^3x\,. \qquad (2\cdot13)$$

The mass M_* is conserved throughout the entire evolution of the system, even if there exists a dissipation process such as the emission of gravitational waves. Thus, when we consider a sequence of constant M_*, it may be regarded as an evolution sequence of the system. We note that E is derived from $M_{\rm ADM}-M_*$ in the second PN order. In the following, we use these quantities to argue the stability property of BNSs. For the sake of convenience, we also define the position of the mass center for each star of binary as

$$x_g{}^i=\frac{1}{M_*}\int\rho_* x^i d^3x\,. \qquad (2\cdot14)$$

In the following section, we use Eqs. (2·12) and (2·13), and substitute the numerical results of ρ, U, and so on, directly into Eqs. (2·12) and (2·13) to estimate E and J. For this case, numerical values of E and J unavoidably involve the higher order PN terms in unexpected forms. Thus, E and J defined above are conserved quantities only in the limit v^2/c^2, U/c^2, $\varepsilon/c^2\ll1$, and otherwise they are not. This point should be kept in mind.

It is also important to note that a solution obtained from Eq. (2·2) is a good approximation of a GR solution only in the case when the PN correction is small. This is because we solve Eq. (2·2) without using the PN expansion, in contrast with the treatment by Chandrasekhar,[11)] and as a result, the solution involves not only correct first PN terms, but also extra higher PN terms, which are not correct terms in general. Thus, a solution obtained from Eq. (2·2) by the above procedure is a correct approximate solution of a GR solution only in the limiting case v^2/c^2, U/c^2, ε/c^2 $\ll1$. Otherwise, it is not the approximate solution in the strict sense.

Finally, we define physical units for the sake of convenience as

$$R_s\equiv\frac{GM_\odot}{c^2}=1.477\ \mathrm{km} \qquad \text{and} \qquad \rho_s\equiv\frac{M_\odot}{R_s{}^3}=6.173\times10^{17}\ \mathrm{g/cm^3}\,, \qquad (2\cdot15)$$

where $M_\odot=1.989\times10^{33}$ g is the solar mass.

§ 3. Numerical results

In this paper, we choose $\Gamma=2$ or 3 as the polytropic exponent. According to models of the EOS for NSs, Γ is $2\lesssim\Gamma\lesssim3$,[15)] so that this assumption is appropriate for a realistic NS. In each case, we define the polytropic constant as

$$K=\begin{cases}2\pi^{-1}Gr_2{}^2 & \text{for}\quad \Gamma=2\,,\\ 2.524\ GM_\odot{}^{-1}r_3{}^5 & \text{for}\quad \Gamma=3\,,\end{cases} \qquad (3\cdot1)$$

where r_2 and r_3 are parameters which are used to adjust the stiffness of the EOS. If we consider a spherical star in the Newtonian theory, r_2 and $a\equiv r_3(M/M_\odot)^{1/5}$, where M

is the mass of the spherical star, become radii of polytropic stars of the polytrope exponents $\Gamma=2$ and 3, respectively.

Since in a previous paper[12] we showed various numerical results for BNSs with $\Gamma=2$, we mainly present numerical results for the $\Gamma=3$ polytrope in this paper. First of all, in Fig. 1, we show the total energy and angular momentum as a function of the orbital separation r_g/a, where r_g denotes the distance between two centers-of-mass, for the Newtonian configuration. In the figures, E and J are shown in units of $E/(GM^2/4a)$ and $J/(G(M/2)^{3/2}a^{1/2})$. The innermost circles (i.e., the circles corresponding to the minimum of r_g/a) denote values where the surfaces of the two members of the binary system come into contact. As in the case $\Gamma=2$,[14),12)] it is found that the minimums of E and J appear at a critical point $r_{\rm crit}$. As pointed out by Lai et al.,[7),8)] this indicates that the secular instability occurs at $r_{\rm crit}$. Since this is not the dynamical instability point, this does not mean that $r_{\rm crit}$ is the radius of the innermost stable circular orbit(ISCO), but it means only that BNSs cannot maintain uniformly rotating orbits if $r<r_{\rm crit}$. However, as shown by Lai et al.,[7),8)] the dynamical instability point will always appear very near the secular instability one, so that we may expect that the ISCO is located at $r \lesssim r_{\rm crit}$.

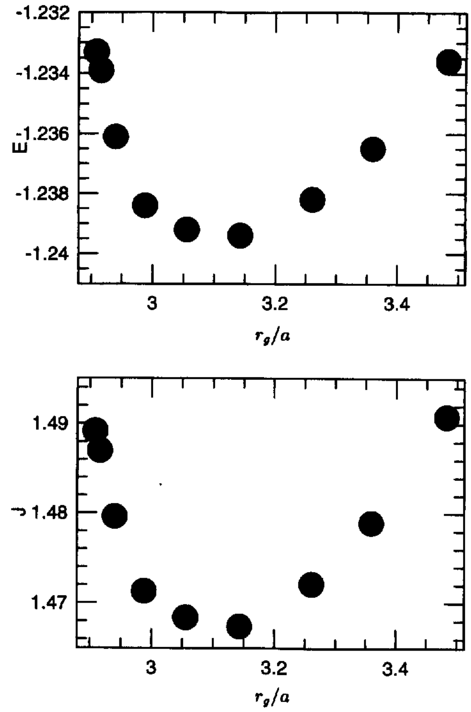

Fig. 1. The energy(E) and the angular momentum (J) as a function of r_g/a for BNSs of $\Gamma=3$ in the Nowtonian case. The energy and the angular momentum are shown in units of $E/(GM^2/4a)$ and $J/(G(M/2)^{3/2}a^{1/2})$. Here, M and a are the total mass of the system and $r_3(M/2M_\odot)^{1/5}$, respectively.

Now, we discuss the stability property of PN configurations. First of all, in Table I, we show several quantities of spherical stars in the PN approximation; r_A is the areal radius, which is defined as

Table I. Various quantities of spherical stars of mass $M_*=1.4\,M_\odot$ for the $\Gamma=3$ polytrope with different polytropic constants (i.e., different r_3) in the PN approximation. r_A and r_e are the areal radius and the coordinate radius, respectively. As mentioned in a previous paper,[12)] the typical error size of each value will be $\sim 0.2-0.3\,\%$.

r_3/R_s	8	9	10	12	15	20
r_A/R_s	8.035	9.087	10.14	12.27	15.45	20.75
r_e/R_s	7.115	8.135	9.170	11.23	14.37	19.61
$M_{\rm ADM}/M_\odot$	1.343	1.346	1.348	1.353	1.358	1.365
$r_A c^2/GM_{\rm ADM}$	5.982	6.752	7.523	9.068	11.37	15.20

$$r_A = r_e\left\{1+\frac{1}{c^2}U(r_e)\right\}, \qquad (3\cdot2)$$

where r_e is the coordinate radius of the spherical stars. From Table I, we see that the PN effect makes the radius of spherical stars small, and this effect is stronger for smaller r_3 (i.e., softer EOS). This property plays an important role in the following discussion. In Fig. 2, we show relations between J and r_g/a_* for BNSs of mass $M_*=2.8\,M_\odot$ and $r_3/R_s=8$, 10, 15 and 40 (filled circles, open circles, filled squares and open squares, respectively) in the PN cases as well as the Newtonian sequence(dotted circles). Note that the Newtonian sequence may be regarded as the case $r_3/R_3\to\infty$ in the PN approximation. Here, $r_g=2|x_g{}^i|$ ($x_g{}^i$ is defined in Eq. (2·14)), and $a_*\equiv r_3(M_*/M_\odot)^{1/5}$. E and J are shown in units of $E/(GM_*^2/4a_*)$ and $J/(G(M_*/2)^{3/2}a_*{}^{1/2})$. Figure 2 shows that the minimums exist at critical value of separations, $r_{\rm crit}$, in each case. As in the case $\Gamma=2$,[12] $r_{\rm crit}$ for PN configurations is $\sim$10−20 % smaller than that in the Newtonian case for realistic models of NSs. This is due mainly to the fact that in the PN approximation, the PN gravity makes the radius of each star of BNSs small compared with the Newtonian case. In reality, we find from Table II that r_e/a_* is $\sim$0.85 for $r_3=8R_s$ and $\sim$0.9 for $r_3=15\,R_s$. This is consistent with the results shown in Fig. 2.

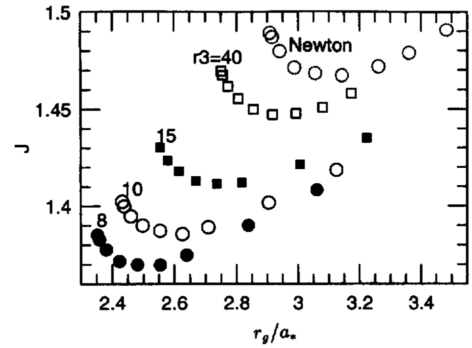

Fig. 2. The angular momentum as a function of r_g/a_* for BNSs with $\Gamma=3$ and several EOSs in the PN approximation. The angular momentum is shown in units of $J/(G(M_*/2)^{3/2}a_*{}^{1/2})$, where $M_*=2.8\,M_\odot$ and $a_*=r_3(M_*/2M_\odot)^{1/5}$, respectively. Filled circles, open circles, filled squares, and open squares denote the PN sequence of $r_3/R_s=8$, 10, 15 and 40, respectively. Dotted circles denote the Newtonian sequence, which way be regarded as the case $r_3/R_s\to\infty$ in the PN approximation.

Let us investigate the influence of this property on $\Omega_{\rm crit}$. In Fig. 3(a), we show the relation between $f\equiv\Omega_{\rm crit}/\pi$, which is the frequency of gravitational waves at $r_{\rm crit}$, and $r_Ac^2/GM_{\rm ADM}$, which denotes the compactness of a spherical star, for BNSs of $M_*=2.8\,M_\odot$. Filled circles and squares denote f for $\Gamma=3$ and 2 in the PN approximation, respectively, and dotted and dashed lines are those in the Newtonian case for $\Gamma=3$ and 2, respectively. Note that in the Newtonian cases, $r_Ac^2/GM_{\rm ADM}=r_ec^2/GM$, and $\Omega_{\rm crit}$ scales as $r_A{}^{-3/2}$. In Fig. 3(b), we also show $f=\Omega_{\rm crit}/\pi$ as a function of r_3/R_s for $\Gamma=3$. It is found that when we compare $\Omega_{\rm crit}$ in the PN approximation with that

Table II. Critical angular velocities ($\Omega_{\rm crit}/\pi$) and separations ($r_{\rm crit}/a_*$) for the $\Gamma=3$ polytrope with different polytropic constants (i.e., different r_3) in the PN approximation. $\Omega_{\rm crit}/\pi$ is shown in units of Hz. Note that the typical error size of each value for $\Omega_{\rm crit}/\pi$ and $r_{\rm crit}/a_*$ is $\sim$1 %.

r_3/R_s	8	9	10	12	15	20	40
$\Omega_{\rm crit}/\pi$(Hz)	970	798	675	504	351	222	75
$r_{\rm crit}/a_*$	2.73	2.78	2.81	2.87	2.95	3.02	3.16

in the Newtonian case, fixing the compactness of NSs or the EOS, the former is always larger than the latter, and for realistic models of $5 \lesssim r_A c^2/GM_{\rm ADM} \lesssim 10$, the deviation is $\gtrsim 100$ Hz. Let us argue the reason for this property in the following.

In the first PN approximation, the angular frequency of two point masses in circular orbits is[3]

$$\Omega = \sqrt{\frac{GM}{r^3}} \left(1 - \frac{3-\eta}{2} \frac{GM}{rc^2}\right), \quad (3\cdot3)$$

where M and η are the total mass of the system and the ratio of the reduced mass to the total mass, respectively. In the case of an equal mass binary system, η is 1/4. Thus, we may write $\Omega_{\rm crit}$ as

$$\Omega_{\rm crit} = \sqrt{\frac{GM}{r_{\rm crit}^3}} \left(1 - \frac{11}{8} \frac{GM}{r_{\rm crit} c^2}\right) + \delta\Omega, \quad (3\cdot4)$$

where $\delta\Omega$ denotes a correction due to the tidal field, the spin angular momentum of each star, and so on.[7] In the following, we regard this as a small quantity. In reality, $\delta\Omega/\Omega_{\rm crit}$ is at most a few % in the Newtonian case.[7),12)]

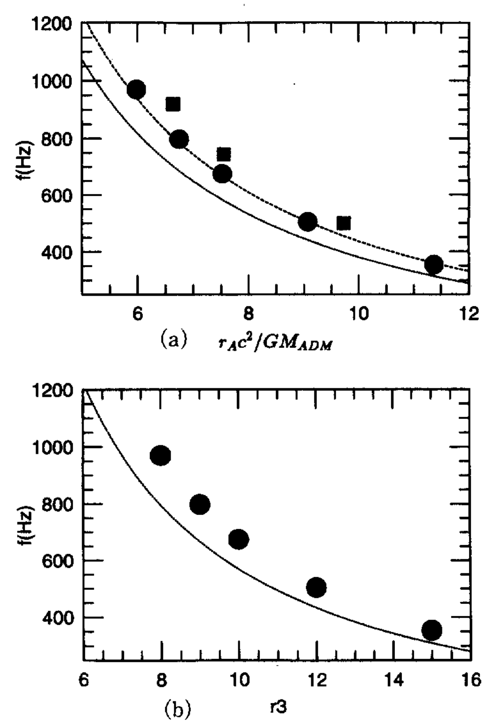

Fig. 3. (a) The frequency of gravitational waves at the critical separation $r_{\rm crit}$, $f = \Omega_{\rm crit}/\pi$, as a function of the compactness of the spherical NS, $r_A c^2/GM_{\rm ADM}$. Filled circles and squares denote f for the PN sequences of $\Gamma = 3$ and 2, respectively. Dotted and dashed lines show f for the Newtonian sequences of $\Gamma = 3$ and 2, respectively.
(b) $f = \Omega_{\rm crit}/\pi$ as a function of r_3/R_s. Filled circles and the dotted line denote f of the PN and Newtonian sequences, respectively.

Since $r_{\rm crit}$ in the PN approximation is smaller than that in the Newtonian case, we can write it as $r_{\rm crit} = r_{{\rm crit},N}(1-\delta)$, where $r_{{\rm crit},N}$ denotes $r_{\rm crit}$ for a Newtonian sequence, and δ is a constant $\sim 0.1-0.2$ which depends on the EOS. Using this expression, Eq. (3·4) is rewritten as

$$\Omega_{\rm crit} \simeq \Omega_{{\rm crit},N} \left(1 + \frac{3}{2}\delta - \frac{11}{8} \frac{GM}{r_{\rm crit} c^2}\right) + \delta\Omega, \quad (3\cdot5)$$

where $\Omega_{{\rm crit},N}$ is $\Omega_{\rm crit}$ for a Newtonian sequence. Present numerical calculations show that the second term in the brackets is always larger than the third term. If we assume that $\delta\Omega$ in the PN approximation is a small correction as in the Newtonian case and it may be safely neglected, $\Omega_{\rm crit}$ is always larger than $\Omega_{{\rm crit},N}$: For $5 \lesssim r_A c^2/GM_{\rm ADM} \lesssim 10$, $\Omega_{\rm crit}$ is $\sim 10-15$ % larger than $\Omega_{{\rm crit},N}$. Although this argument is very rough, it seems essentially to explain the quantitative difference between $\Omega_{\rm crit}$ and $\Omega_{{\rm crit},N}$.

Finally, to check the applicability of the first PN approximation to this problem, in Fig. 4 we show the relation between $\Omega_{\rm crit} a_*^{3/2}(M_*/2)^{-1/2}$ and $GM_{\rm ADM}/r_A c^2$ for BNSs of mass $M_*=2.8\,M_\odot$. In the first PN approximation every quantity should behave approximately as

$$\text{(Newtonian order quantity)} + \frac{GM_{\rm ADM}}{r_A c^2}\times\text{(PN correction)}. \qquad (3\cdot6)$$

Hence, in order to check the applicability of the first PN approximation it is a good test to see whether this relation holds or not. From Fig. 4, we find that for $GM_{\rm ADM}/r_A c^2 \lesssim 0.1$, a linear relation such as Eq. (3·6) holds, but for $GM_{\rm ADM}/r_A c^2 \gtrsim 0.1$ it does not. Hence, the first PN approximation is good only for the case when each NS of BNSs is not extremely compact, $GM_{\rm ADM}/r_A c^2 \lesssim 0.1$; according to a realistic NS model,[15] $0.14 \lesssim GM_{\rm ADM}/r_A c^2 \lesssim 0.2$, so that the solution in the first PN approximation is not accurate enough as an approximate solution of a fully GR configuration. To investigate the stability property of a realistic BNS, we need to include further PN corrections, such as second PN corrections.

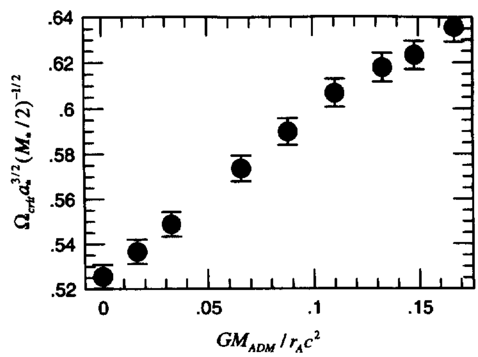

Fig. 4. $\Omega_{\rm crit}(a_*^3/(M_*/2))^{1/2}$ as a function of the compactness of NS, $GM_{\rm ADM}/r_A c^2$, for BNSs of mass $M_*=2.8\,M_\odot$. The error bar is drawn to represent typical error size, ~1%. We can see that for $GM_{\rm ADM}/r_A c^2 \lesssim 0.1$, the linear relation between the two quantities approximately holds. Otherwise, it does not. This implies that the first PN approximation is sufficient as the approximation of a fully GR configuration only for the case $GM_{\rm ADM}/r_A c^2 \lesssim 0.1$.

§ 4. Summary

Making use of solutions of the equilibrium configuration for synchronized BNSs which are obtained by means of the numerical method developed in a previous paper,[15] we have considered the stability property of BNSs just before the merging. Our conclusions are as follows.

(1) As in the Newtonian case, in the PN approximation, the secular instability for synchronized BNSs of a realistic EOS (i.e., $\Gamma=2\sim3$ and r_2 or r_3 $(M_*/M_\odot)^{1/5}\simeq 10-15$ km) will occur at a critical angular frequency $\Omega_{\rm crit}$ before the surfaces of the two NSs of a binary system come into contact.

(2) When we compare $\Omega_{\rm crit}$ in the PN approximation with that in the Newtonian case, fixing the compactness of each NS (i.e., $GM_{\rm ADM}/r_A c^2$) or the EOS, the PN value is 10-15 % larger than the Newtonian value for realistic BNSs.

(3) The reason for the result (2) is mainly that the PN effect makes the radius of each NS smaller than that for the Newtonian case.

In particular, we would like to emphasize the result (3): the effect of the first PN correction to each NS of a binary system is very important to determine $\Omega_{\rm crit}$ of BNSs just before merging. Recently, Lai and Wiseman[16] obtained the ISCO of BNSs. In their approach, they tried to determine the ISCO of BNSs using the hybrid equation of motion (EOM)[17] incorporating the tidal effect of each NS of BNSs into the EOM.

Also, Ogawaguchi and Kojima[18] calculated the orbital evolution of BNSs just before the merging using a similar procedure to Lai and Wiseman. Their results are worth noting because they took into account the GR effects as well as the tidal effects. However, they took into account the relativistic effect only of the orbit, and they did not consider the relativistic correction to the tidal effect (i.e., relativistic correction to the configuration of each NS). As we pointed out above, the relativistic effect on the two NSs of a BNS system will play a role as important as the relativistic effect on the orbit in determining the critical stability point. Therefore, their treatments will not be accurate enough.

Finally, we briefly discuss the implication of our present results to the location of the ISCO. As mentioned above, $r_{\rm crit}$ denotes the point where the secular instability occurs, so it does not denote the point of the ISCO. The ISCO will be determined by the dynamical instability point. However, the above simple argument for the frequency shift of the secular instability point due to the PN correction seems to hold for the frequency at which the dynamical instability occurs, $f_{\rm dyn}$. Thus, we may expect that the PN corrections will shift $f_{\rm dyn}$ to a larger value overall.

Acknowledgements

For useful discussions and comments, the author thanks H. Asada, Y. Kojima, D. Lai, T. Nakamura, M. Sasaki and T. Tanaka. Numerical calculations were partly performed on FACOM VP-2600 of the Data Processing Center of Kyoto University. This work was in part supported by the Grant-in-Aid on Scientific Research of the Ministry of Education, Science and Culture, No. 07740355.

References

1) A. Abramovici et al., Science **256** (1992), 325.
K. S. Thorne, in *Proceedings of the 8-th Nishinomiya-Yukawa Memorial Symposium on Relativistic Cosmology*, ed. M. Sasaki (Universal Academy Press, Tokyo, 1994), p. 67.
2) C. Bradaschia et al., Nucl. Instrum. Method Phys. Res. Sect. **A289** (1990), 518.
3) C. M. Will, in *Proceedings of the 8-th Nishinomiya-Yukawa Memorial Symposium on Relativistic Cosmology* (Ref. 1)), p. 83.
4) C. Cutler et al., Phys. Rev. Lett. **70** (1993), 2984.
5) X. Zhuge, J. M. Centrella and S. L. W. McMillan, Phys. Rev. **D50** (1994), 6247.
6) L. Lindblom, Astrophys. J. **398** (1992), 569.
7) D. Lai, F. A. Rasio and S. L. Shapiro, Astrophys. J. Suppl. **88** (1993), 205.
8) D. Lai, F. A. Rasio and S. L. Shapiro, Astrophys. J. **420** (1994), 811; Astrophys. J. Lett. **406** (1993), L63.
9) S. Chandrasekhar, *Ellipsoidal Figures of Equilibrium* (Dover, NY, 1987).
10) C. S. Kochanek, Astrophys. J. **398** (1992), 234.
L. Bildsten and C. Cutler, Astrophys. J. **400** (1992), 175.
11) S. Chandrasekhar, Astrophys. J. **148** (1967), 621.
12) M. Shibata, Osaka University Preprint, OU-TAP 26, submitted to Phys. Rev. **D**.
13) S. Chandrasekhar, Astrophys. J. **142** (1965), 1488.
14) F. A. Rasio and S. L. Shapiro, Astrophys. J. **401** (1992), 226; **432** (1994), 242.
15) For example, S. L. Shapiro and S. A. Teukolsky, *Black Holes, White Dwarfs and Neutron Stars* (NY, Wiley, 1983).
16) D. Lai and A. G. Wiseman, private communication.
17) L. E. Kidder, C. M. Will and A. G. Wiseman, Phys. Rev. **D47** (1993), 3281.
18) W. Ogawaguchi and Y. Kojima, submitted to Prog. Theor. Phys.